INTERFACE

rsif.royalsocietypublishing.org

Research

Cite this article: Kunita I, Yamaguchi T, Tero A, Akiyama M, Kuroda S, Nakagaki T. 2016 A ciliate memorizes the geometry of a swimming arena. *J. R. Soc. Interface* **13**: 20160155.
http://dx.doi.org/10.1098/rsif.2016.0155

Received: 22 February 2016
Accepted: 20 April 2016

Subject Category:
Life Sciences–Mathematics interface

Subject Areas:
biomathematics, computational biology, biophysics

Keywords:
memory, ion channel, tetrahymena, mathematical modelling, Hodgkin Huxley equation

Author for correspondence:
Toshiyuki Nakagaki
e-mail: nakagaki@es.hokudai.ac.jp

Electronic supplementary material is available at http://dx.doi.org/10.1098/rsif.2016.0155 or via http://rsif.royalsocietypublishing.org.

THE ROYAL SOCIETY PUBLISHING

A ciliate memorizes the geometry of a swimming arena

Itsuki Kunita[1], Tatsuya Yamaguchi[2], Atsushi Tero[2,3], Masakazu Akiyama[1], Shigeru Kuroda[1] and Toshiyuki Nakagaki[1]

[1]Research Institute for Electronic Science, Hokkaido University, N20W10, Kita-Ward Sapporo 001-0020, Japan
[2]Graduate School of Mathematics, and [3]Institute of Mathematics for Industry, Kyushu University, 744 Motooka, Nishi-ku, Fukuoka 819-0395, Japan

Previous studies on adaptive behaviour in single-celled organisms have given hints to the origin of their memorizing capacity. Here we report evidence that a protozoan ciliate *Tetrahymena* has the capacity to learn the shape and size of its swimming space. Cells confined in a small water droplet for a short period were found to recapitulate circular swimming trajectories upon release. The diameter of the circular trajectories and their duration reflected the size of the droplet and the period of confinement. We suggest a possible mechanism for this adaptive behaviour based on a Ca^{2+} channel. In our model, repeated collisions with the walls of a confining droplet result in a slow rise in intracellular calcium that leads to a long-term increase in the reversal frequency of the ciliary beat.

1. Introduction

The behaviour of protozoa has been examined for over a hundred years under various external conditions and has been compared with intelligent behaviour in higher animals [1–8]. It has long been observed that even protozoa behave in a highly adaptive way towards complicated environmental conditions [9–15]. These reports have repeatedly stimulated discussion on the possibility of something like primitive intelligence. The adaptability of protozoa and its ethological implications has become a classical topic, but much still remains to be understood.

Because of the relative simplicity of unicellular systems compared with multicellular organisms, the physical mechanism of adaptation may be easier to clarify. Insight has been provided by a number of studies such as solving a maze [16] and anticipating periodic environmental events by the slime mould *Physarum* [15]. These observations encourage us to rethink how this capacity for adaptation develops from the physical nature of the organism.

Concerning the capacity to learn the geometry of a space, impressive pioneering work on a protozoan ciliate *Paramecium* was performed by Bramstedt in 1935 [17]: after the organism was transferred from a tiny container to a large container, it swam freely but followed a trajectory that was similar to the shape of its previous container. Although this finding was striking, some other research groups carefully re-examined it and drew negative conclusions [18,19]. Here we attempt to throw more light on memory capacity of this type.

In this report, we design a new quantitative experiment and confirm that another species of ciliate *Tetrahymena* shows the capacity to learn spatial configurations. We first carry out a qualitative characterization of the adaptive behaviour. We then propose a possible physical mechanism for this type of memory capacity in ciliates, based on the regulation of electric phenomena in the membrane that are closely coupled with ciliary motion. Finally, we discuss the implications of this memorizing capacity from the perspective of comparative ethology.

2. Organism and methods

Protozoan ciliates *Tetrahymena* were cultured in a liquid medium (KCl 8 mg l^{-1}, $MgSO_4$ 8 mg l^{-1}, $CaCl_2$ 8 mg l^{-1}) and incubated in a dark room at room

temperature (23–25°C). After being allowed to swim in a wide space freely for several tens of minutes, specimens of *Tetrahymena* were confined in a spherical droplet of culture medium (0.3–0.6 mm in diameter (ϕ), approximately 0.014–0.11 µl) embedded in mineral oil for 15 min. Next, the specimens were transferred to the much larger space of a Petri dish (35 mm in diameter, 3 ml of medium).

To minimize any space-dependent effects of unknown chemicals that may be released from the organism during swimming in the droplet, the liquid medium was thoroughly mixed just after the organism was transferred from the droplet to the Petri dish. The specimens then began to swim freely.

The swimming motion of *Tetrahymena* was monitored under dark-field illumination using a stereoscopic microscope (Olympus, SZX16). Microscopic images were captured using a CCD camera and recorded on video. The recorded images were transferred and saved on a personal computer. Using customized software, we analysed the swimming trajectories of *Tetrahymena* by the conventional method of video image analysis.

To characterize a swimming trajectory, the maximum distance (MD) was defined as $\mathrm{MD}(t) = \max\{\sqrt{(x(t)-x(t+h))^2+(y(t)-y(t+h))^2} \mid -\tau \le h \le \tau\}$, where $(x(t), y(t))$ is the position of organism at time t. MD was plotted as a function of τ and could saturate at some value of diameter when the swimming trajectory was circular. At last, statistical occurrence of MD was plotted in the function of τ. Numbers of cells were 34 ($\phi = 0.3$ mm), 31 (0.4 mm), 30 (0.5 mm) and 22 (0.6 mm).

For statistical confirmation of spatial extent of swimming trajectory after the confinement, the width of the circular shape of trajectory (approximate diameter) was measured for each circular shape on the whole trajectory of swimming, and the normalized frequency was plotted. The numbers of circles were 757 ($\phi = 0.3$ mm), 292 (0.4 mm), 375 (0.5 mm) and 76 (0.6 mm).

3. Adaptive behaviour towards the shape and size of a swimming space in *Tetrahymena*

In an open space, *Tetrahymena* usually swam in a straight line at a velocity of 0.81 ± 0.27 mm s^{-1} (mean $\pm$ s.d., $N = 30$), and changed the direction of swimming at a frequency of 0.01–0.1 Hz, as shown in figure 1*a*1.

Figure 1*a*2–*a*4 shows the swimming trajectories observed in a tiny spherical droplet (the diameter, ϕ, is 0.3 mm): *Tetrahymena* repeatedly turned at the droplet wall and moved closely (figure 1*a*2) or approximately (figure 1*a*3) along the wall, and sometimes in a different manner (figure 1*a*4). The swimming patterns (figure 1*a*2 and figure 1*a*3) were often observed in this confined space over a few minutes. The pattern of swimming changed on a longer time scale.

After the organism was transferred from the confined space to a wide, open space, the swimming trajectory repeatedly traced a circular shape that was similar to the previous confined space (figure 1*a*5,*a*6). Sometimes the organism swam for a period of time almost in a straight line or in a large arc of much lower curvature; occurrences of these modes of swimming are apparent in the trajectories in figure 1*a*5,*a*6. The adaptive trajectory lasted from a few minutes to an hour, and the duration time differed from one individual to the next. The statistical occurrence of this type of trajectory was 45%, and the occurrence of swimming similar to figure 1*a*1, in which there was no adaptive change in the trajectory, was 53%, in a total of 117 specimens summing up the different ϕs (0.3, 0.4, 0.5, 0.6 mm). The remaining of cases were the other types. The duration of confinement was too short at 5 min to observe the type in figure 1*a*5,*a*6, and too long at 30 min (70% of organisms tended to stop moving).

Figure 1*b*1–*b*3 shows the characterization of swimming type. In a segment of swimming trajectory extracted in the time interval of 2τ, the statistical occurrence of MD of any two positions along the segment was measured with respect to τ. In the type in figure 1*a*5, MD was saturated at 0.4 mm as the trajectory is approximately circular at a diameter of 0.4 mm (figure 1*b*2). Such saturation was not observed in figure 1*b*1 when the trajectory was almost straight like figure 1*a*1. The trajectory was somewhere in between, like figure 1*a*6, as shown in figure 1*b*3.

For modes of swimming shown in figure 1*a*5 and *a*6, normalized frequencies of the diameters of the circular trajectories (excluding periods of time in which the organism swam in a straight line or wide arc) were determined and are shown in figure 1*c*. The diameter of the swimming trajectory increased with the diameter of the confined space experienced, which varied from 0.3 to 0.6 mm. The diameter of the swimming trajectory increased with ϕ and was approximately 1.3 times larger than ϕ (figure 1*d*). We are at present unable to explain this difference, and it is unclear whether the difference is physiologically significant.

In the control group that did not experience the confined space, only fewer than 10 times of the circular trajectories were counted when 80 individuals were traced for 1 min, and their diameters ranged from 1 to 2 mm. So the circular trajectory in the diameter of less than 1 mm was not observed at all for the accumulated 80 min of observation time. By contrast, after the experience of confined space, the numbers of circular trajectory (the diameter was mainly less than 1 mm) were 757, 292, 375 and 76 for the accumulated total observation time of 38 min, 15 min, 26 min and 23 min for droplet diameters of 0.3 mm, 0.4 mm, 0.5 mm and 0.6 mm, respectively. Therefore, we concluded that a circular trajectory less than 1 mm did not result from some stochastic fluctuations of swimming trajectory but was clearly induced by the confinement.

For the data of diameter distribution shown in figure 1*c*, the statistical significance tests of non-parametric type were done. It is because a precondition of equal variance for parametric ANOVA and multiple comparison tests was not satisfied: the variance of each group (different size of confined space) was not equal using Bartlett's test for equal variance. By means of non-parametric Kruskal–Wallis test, the medians varied significantly among the groups ($p < 0.0001$), and the rank sum differed significantly between any pair of groups ($p < 0.05$) by Dunn's multiple comparison test. Therefore, we concluded that the diameter of trajectory induced by the confinement differed significantly in the groups.

The swimming speed also changed while the swimming trajectory was circular: for instance, when $\phi = 0.3$ mm, 0.39 ± 0.12 (mean $\pm$ s.d., $N = 14$) in the droplet and 0.56 ± 0.16 after the confinement. In the other diameters, the speeds after the confinement were 0.51 ± 0.09 ($\phi = 0.4$ mm), 0.61 ± 0.13 ($\phi = 0.5$ mm) and 0.49 ± 0.09 ($\phi = 0.6$ mm).

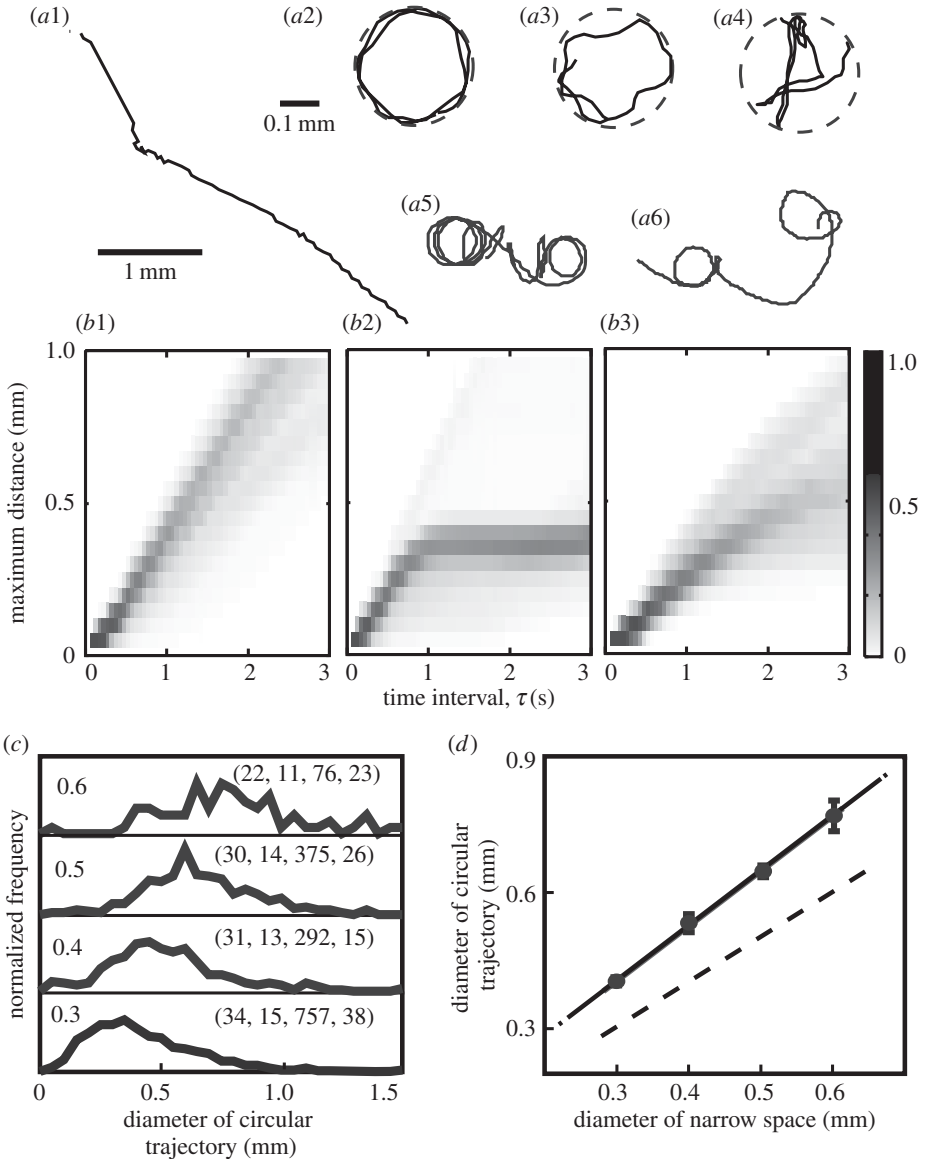

Figure 1. Typical swimming trajectories of *Tetrahymena* before and after the confinement: (*a*1) in a wide, open space before confinement in a small space; (*a*2–*a*4) in the confined space of a spherical droplet of diameter 0.3 mm; (*a*5, *a*6) in an open space after confinement. Solid and dashed lines show the trajectories of swimming and the shape of the confined space, respectively. (*b*1–*b*3) Statistical occurrence of maximum distance (MD) in the function of τ at the diameter of droplet, 0.3 mm. Grey level indicates a normalized frequency according to the grey chart on the right. (*c*,*d*) Dependence of the diameter of circular motion on the diameter of the confined space experienced, re-drawn from (*c*). The left numbers in each panel of (*c*) indicate the diameters of the confined space (mm), and the numbers in parentheses on the right indicate the number of experiments, number of results of type (*a*5), (*a*6), number of circular trajectories count, total observation time in minute for counting the circular trajectory. The error bars in (*d*) represent the standard error. The dashed line indicates where the two diameters are equal. Number of results of type (*a*5), (*a*6) (diameter of droplet, mm): 15(0.3), 13(0.4), 14(0.5), 11(0.6).

4. A mathematical model for adaptive behaviour to a confined space

The swimming of a ciliate is driven by the collective motion of many cilia, which is controlled by the membrane potential and the Ca^{2+} current [6,20–22]. When the anterior part of a ciliate collides with an obstacle, Ca^{2+} ions flow into the cell and lead to reversal of the ciliary beat. The ciliate then changes direction and the turning angle depends on the period over which Ca^{2+} exceeds the threshold concentration [23]. A spontaneous turn sometimes occurs without collision with the wall due to excitation of the membrane evoked by internal and external fluctuations [24–28].

Based on the biochemical process that controls swimming, we propose a simple mathematical model. Let a ciliate be represented by a point particle with position $(x(t), y(t))$ at time t. The swimming motion can then be described as $(\dot{x}, \dot{y}) = (\bar{v}\cos\theta(t), \bar{v}\sin\theta(t))$, where $\bar{v}$ is the speed (constant) and $\theta(t) \in [-\pi, \pi]$ is the measured angle of the swimming direction with respect to the x-axis, as shown in figure 2*a*1.

Next, we describe the motion when the cell comes into contact with the vessel wall: the ciliate moves along the wall without any frictional resistance. That is, it slips along the wall. As shown in figure 2*a*2, the swimming trajectory is then given by the projection of the hypothetical free motion (in the case of no wall) onto the vessel wall, which is $(\dot{x}, \dot{y}) = (\bar{v}\cos\varphi(t)\cos\psi(x, y), \bar{v}\cos\varphi(t)\sin\psi(x, y))$, where $\psi(x,y) \in [-\pi, \pi]$ is the angle of the vessel wall at the contact point with the cell and $\varphi(t) \in [0, \pi/2]$ is the contact angle between the vessel wall and the direction of hypothetical free motion of the cell.

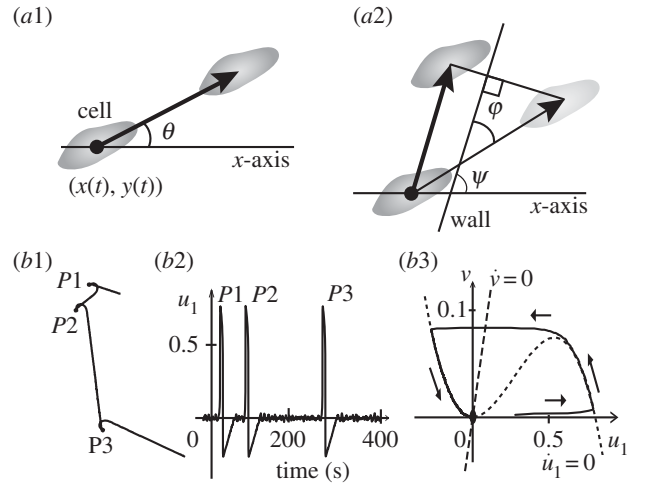

Figure 2. Schematic of mathematical description of swimming motion for free swimming (*a*1) and when in contact with the vessel wall (*a*2). Simulation of normal free swimming in the case of an excitable u_1 (*b*1–*b*3). (*b*1) Typical trajectory of swimming. (*b*2) Time course of u_1. The noise-induced spikes *P*1, *P*2 and *P*3 correspond to the turning events *P*1, *P*2 and *P*3, respectively, in (*b*1). (*b*3) A typical trajectory of a spike in the state space of u_1 and *v*. The solid line is the solution trajectory, and the dotted and the dashed lines are the null clines for u_1 and *v*, respectively.

Here we assume that the angle of turning is proportional to the Ca^{2+} influx such that $\dot{\theta} = b_0u_0(t) + b_1u_1(t)$, where u_0,u_1 are gating variables of the Ca^{2+} influx with slow and fast time scales, respectively. The existence of two such time scales for gating was suggested by experiment [29] and the molecular details have been well discussed for other types of cells such as neurons [30,31].

As the mechano-sensitive Ca^{2+} channel is located only at the anterior end in *Paramecium* [20], we set the threshold angle (φ_0) of collision sensitivity as the smallest angle at which the collision evokes a Ca^{2+} influx. However, the actual value of φ_0 is not well known although the estimated φ_0 could be within the range of 30° to 60° in *Paramecium*. Therefore, we examine the effects of φ_0 as a model parameter.

The slow variable $u_0(t)$ is given by $\dot{u}_0 = -\varepsilon u_0 + \delta(\varphi)s$, where ε is a small positive value ($\varepsilon = 0.0001$). The parameter δ is the indicator of collision and takes a value of 1 (when colliding and $\sin(\varphi) > \sin(\varphi_0)$) or 0 (otherwise). The parameter *s* is a constant that expresses the small effect of a collision on the gating ($s = 0.003$). Because this slow gate opens a little in response to a collision and then closes slowly, a series of frequent collisions can be accumulated and a long-term effect on the regulation of the swimming direction appears. The dynamics of this slow variable is the new and most important idea in our model.

The fast variable u_1 shows excitable and oscillatory behaviour and is linked to another variable $v(t)$ by FitzHugh–Nagumo type equations [32], $\tau_u\dot{u}_1 = -u_1(u_1 + a_1)(u_1 + a_2) - v + Iu_0 + \xi_{u_1}(t)$ $\tau_v\dot{v} = a_3u_1 - v + \xi_v(t)$. Here $\tau_v > 1 \gg \tau_u > 0$, a_1, a_2 and *I* are the parameters and $\xi_{u_1}(t)$, $\xi_v(t)$ are random variables.

Lastly, we summarize the general framework of the model. The regulation of swimming direction is a function of Ca^{2+} influx that can be described by some of the gating variables of ion channels. It is likely that the full dynamics of the membrane potential includes many types of channel, but the effective modes of the dynamics can be described by just one or a few variables when the system is perturbed around the resting state of the potential by the stimulation of a collision. If the perturbed state is not far from the resting state (for free straight swimming, and $(u_0, u_1) = (0, 0)$), the linear approximation assumed in the u_0-equation of our model may be acceptable. Although the molecular machinery of the Ca^{2+} channels is not yet fully understood, it is expected that the mathematical description in our model is still plausible on a general level.

5. Numerical simulation of the model

Figure 2*b* shows the simulation of normal free swimming without any collision with the wall when u_1 is in an excitable regime. Typical trajectories of swimming look like a combination of straight motion and stochastic turning (figure 2*b*1). This turning results from a fluctuation-induced spike of u_1. The spikes *P*1, *P*2 and *P*3 in the time course of u_1 (figure 2*b*2) correspond to the three turning events *P*1, *P*2 and *P*3, respectively, in figure 2*b*1. A typical trajectory of a spike in the state space of u_1 and *v* is shown in figure 2*b*3.

Figure 3 shows the results of simulation ($\phi_0 = 40°$) for two different sets of parameters: an excitable u_1 (figure 3*a*1–*a*3) and an oscillatory u_1 (figure 3*b*1–*b*3). The simulated trajectories of swimming are similar to the real ones (figure 1) during (figure 3*a*1,*b*1) and after (figure 3*a*2, *b*2) confinement in the small space.

At the initial condition (time 0), the organism contacts the wall at an angle of 90°, and the next time-step changes its direction of movement a little because $\varphi > \varphi_0$. This slight change in direction continues with further collisions as long as $\varphi > \varphi_0$, and the contact angle φ decreases to φ_0 (figure 3*a*3).

While the contact angle gradually decreases, u_0 increases by *s* (=0.003) at each change of direction and continues to increase over a series of frequent turning events as the decay rate of u_0 is slow. The increase in u_0 implies that the swimming trajectory becomes ever more curved.

Around the saturation level of u_0 at φ_0, the curvature of swimming becomes constant while the frequency of active turning and the decay speed of u_0 become balanced. This simulated trajectory (figure 3*a*1) is similar to that observed experimentally (figure 1*a*2). This saturated state of u_0 is maintained for some time after the vessel wall is removed at time 900 in the simulation, and the simulated (figure 3*a*2) and experimental (figure 1*a*5) trajectories remain similar.

Surprisingly, the diameter of circular motion after confinement is 1.3 times larger than that of the confined circular space, as also observed for the real organism. This relationship was reproduced for confined spaces with a range of sizes (figure 3*c*), provided that $\varphi_0 = 40°$. This adaptive circular motion slowly disappears (much later than time 1500) and straight motion is recovered ($u_0 = 0$, data not shown).

The simulation described above was performed in the excitable regime of u_1 and noise-induced spikes of u_1 were observed. These spikes result in a transient modulation of the curvature of swimming trajectory.

In the alternative regime of oscillatory u_1, the basic behaviour of u_0 observed for excitable u_1 was reproduced, even though regular oscillations of φ and u_1 are involved. The simulated trajectory during (figure 3*b*1) and after (figure 3*b*2) confinement are similar to the experimental trajectories in figure 1*a*3 and *a*6 with respect to the circular motion and its modulation.

As shown in figure 3*c*, the simulated diameters of free motion were approximately 1.3 times larger than the

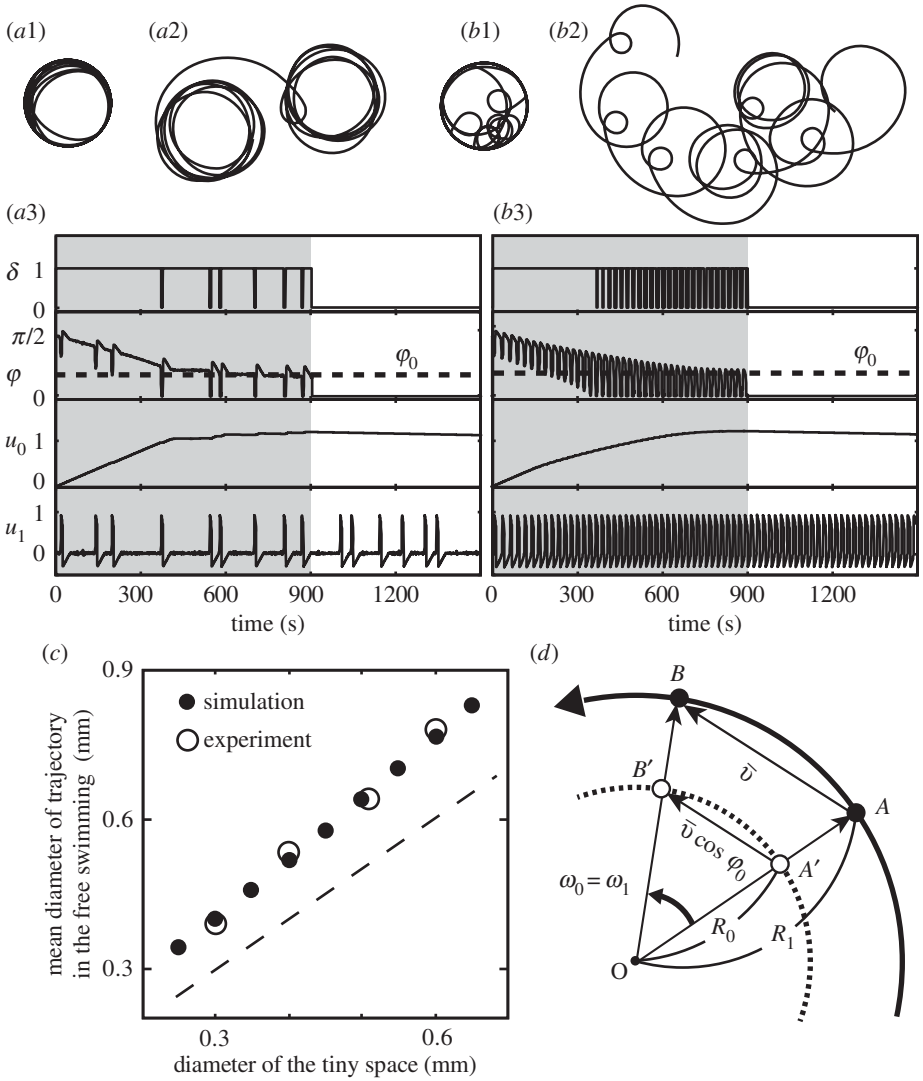

Figure 3. Mathematical modelling for swimming behaviour during and after confinement. Numerical simulations in the case of excitable u_1 ($I = 0.0$)(*a*1–*a*3) and in the case of oscillatory u_1 ($I = 0.15$)(*b*1–*b*3). Trajectories during (*a*1,*b*1) and after (*a*2,*b*2) the confinement. Time courses of key variables (*a*3,*b*3) and the confinement ended at time 900. The parameters for both cases were as follows: vessel size = 0.2 mm, $\bar{v} = 0.3$ mm s^{-1}, $\varepsilon = 0.0001$, $s = 0.003$, $\tau_u = 0.0025$, $\tau_v = 20$, $a_1 = -0.3$, $a_2 = -1$, $a_3 = 4$, $b_0 = 1$, $b_1 = 5$, $\varphi_0 = 40^\circ$ and $\xi_{u_1}, \xi_v \in [-0.25, 0.25]$. (*a*1,*a*2,*b*1,*b*2) Drawn to the same scale. (*c*) Simulated relationship between the diameter of the confined space and that of the circular trajectory just after confinement. The dashed line indicates where the two diameters are equal. All parameters were the same as (*c*). (*d*) Schematic of geometrical analysis of the relationship between the two diameters. See the main text for details.

diameter of the confined space when $\varphi_0 = 40^\circ$. This can be understood from the following geometrical analysis, as illustrated in figure 3*d*. Here we neglect u_1 because u_0 is essentially important to persist in the circular motion. As the trajectory of free swimming (the thick solid line in the figure) is circular due to the constant value of $\dot{\theta}$ (u_0 is nearly constant), we set the point O at the centre of this circle and denote the angular velocity as ω_1. When the organism is confined in the small space (indicated by the dashed line), the trajectory of free swimming is projected onto the dashed line. The velocity vectors, $\boldsymbol{AB}$ between points A and B and $\boldsymbol{A'B'}$ between points A' and B', are $(\bar{v}\cos\theta, \bar{v}\sin\theta)$ and $(\bar{v}\cos\varphi\ \cos\psi, \bar{v}\cos\varphi\ \sin\psi)$, respectively. The lengths $|\boldsymbol{AB}|$ and $|\boldsymbol{A'B'}|$ are thus given by $\bar{v}$ and $\bar{v}\cos\varphi$, respectively. The angular velocity shortly before and after the end of confinement can be approximated (for small Δt) by $\omega_0 \simeq \bar{v}\cos\varphi_0/R_0$ and $\omega_1 \simeq \bar{v}/R_1$, respectively, where R_0 and R_1 are the radii of the circular trajectories during and after confinement. Because ω_1 is equal to ω_0, the ratio of the radii is given by $R_1/R_0 = 1/\cos\varphi_0$, which is 1.3 in the case of $\varphi_0 = 40^\circ$.

6. Discussion

As the confinement in a tiny droplet is an artificial condition, one may wonder if there indeed is such a space in the wild and if the circular swimming pattern observed is actually physiologically meaningful. Careful discussion on this matter is needed.

In stagnant waters like shallow rice paddy fields and ponds which are typical habitats for ciliates, there may be dense aggregates of fibrous algae like *Spirogyra* that form three-dimensional meshes with many tiny cavities. Or there may be aggregates of debris at the bottom of the paddy field or pond that look like media with many small-scale pores. Although the exactly spherical shape examined in this report is hardly possible under such natural conditions, cavities whose shape can be approximated by deformed spheres are to be expected. In this sense, a capacity to adapt to a confined spaces is not meaningless.

On the other hand, let us assume that there is no such cavity in the wild. Organism possess a high-enough capacity to adapt to a shape never experienced before. This, in turn, infers that

Tetrahymena has generalized capacity for spatial memory. Whether or not spherical cavities occur naturally, the adaptive capacity reported here is of potential physiological usefulness.

When we confined them for more than 30 min, we observed that 70% of the individuals after exhibiting a circular trajectory stopped all movement. One may argue that the experimental conditions were stressful to the organisms. A different interpretation, however, is possible. In order to avoid frequent contacts with the wall, it may be favourable to cease movement, which would constitute an adaptive behaviour. As the organisms started to swim again sometime after the confinement, we can exclude a weakening of its physical condition by the confinement.

The adaptive behaviour reported here is of time scale shorter than a life span, and much shorter than multiple generations. It may be expected that complicated geometries of real micro-habitats are exerted in the wild. Possible advantages of this capacity will be examined in the future.

In the mathematical modelling performed in this paper, we assumed that Ca^{2+} and their Ca^{2+} channels played the key role, as many previous papers on the electrophysiological regulation of swimming behaviour in ciliates strongly suggested their importance [6,20,22,23]. This does not mean that Ca^{2+} and Ca^{2+} channels indeed contribute to the development of the adaptive behaviour reported in this paper. Therefore, this point awaits experimental verification.

The mathematical model proposed here, however, will still hold in a mathematical sense even if the key molecules are not Ca^{2+} and Ca^{2+} channels, because we assumed only two things (i) slower elicitation of a response that can accumulate their repetitive stimulation and (ii) dependency of the response sensitivity on the contact angle. The first assumption needs to be examined biologically and mathematically.

The key assumption in our model is the slow regulation of the Ca^{2+} channel, which is supported by reports that the shutdown of the Ca^{2+} current in *Paramecium* involves fast (10 ms range) and slow (10–100 s range) kinetics [29], and that such slow dynamics of the Ca^{2+} current is also widely found in both invertebrate and vertebrate neurons. It is thus plausible that adaptation and memorizing at the level of the cell might be embedded in the slow dynamics of channel motion. The adaptive capacity observed in this report is maintained for some time after the experience of confinement, and this might result in some benefit to the organism.

The swimming speed decreased down to 0.39 ± 0.12 in the droplet (the diameter is 0.3 mm) in comparison with 0.81 ± 0.27 in the wide-open space before being confined, and increased up a little to 0.56 ± 0.16 in the wide-open space after being confined. This change in the swimming speed is consistent with the well-known correlation between the swimming speed and curvature of swimming trajectory in *Paramecium* [21]: the swimming speed slows down while the curvature of swimming trajectory is larger, due to the increase in intracellular Ca^{2+} concentration which is induced by change in K^+–Ca^{2+} composition of external medium. Although the species of organism is different from *Tetrahymena*, it is known that the swimming trajectory is circular in the diameter of 0.2–0.8 mm when the swimming speed is one-half or more slower than the normal speed (0.8–1.2 mm s^{-1}), and that the diameter is smaller at the slower swimming speed. This relationship of diameter and speed was very similar to the results observed in our experiment.

It is noted that a ciliate *Paramecium* is capable of swimming in a circular trajectory in a wide-open space under the specific conditions of external medium. This capacity can contribute to the space memory of spherical shape. Then a question arises: what kinds of shape other than spheres does the ciliate memorize? The original research done by F. Bramstedt showed a triangle was a possibility [17]. To test various shapes of arena is very interesting.

The capacities of adaptation and memory are of interest in basic biology and comparative ethology. In the field of neuroscience of higher animals, molecular events involved in the long- and short-term potentiation of synaptic connections in neural circuits have been studied in relation to the involvement of the *N*-methyl-*d*-aspartate receptor (NMDA receptor). Even in protozoa, like *Paramecium* and *Tetrahymena*, the NMDA receptor plays a key role in the regulation of swimming behaviour by modulating the membrane potential and the Ca^{2+} influx/efflux across the membrane [30,31]. This similarity implies a common evolutionally origin of capacity of memory and adaptation between ciliates and higher animals.

The range of time periods over which the real organisms exhibited the circular trajectories varied from minutes to hours. This large variation may be explained through the mathematical model. In the model, the time derivative of the slow variable u_0 is just proportional to $-\epsilon u_0$ as this is assumed to be the first order approximation of much more complicated dynamics for real channel molecules. The values of the proportional constant ϵ might be distributed over a range of 10-fold difference. Or, the complicated dynamics of real-world mechanism might be sensitive to internal and/or external noise through a nonlinear effect of dynamical motion.

Many types of smart behaviour in ciliates have been reported over the past 100 years. The capacity of conditioning (associative learning in response to two different stimulations) is one example. Even this type of higher learning capacity might be explained by a study of channel behaviour. This paper suggests a promising future direction for research on the *physical ethology* of ciliates.

Competing interests. We declare we have no competing interests.

Funding. This research was supported by JSPS KAKENHI grant nos. 25730178 (I.K.), 24120709 (A.T.), 20300105 (T.N.) and 26310202 (T.N.), by a Grant-in-Aid for Scientific Research on Innovative Area from MEXT (25111726 (T.N.), 25103006 (T. N.)) and by the Strategic Japanese-Swedish Research Cooperative Program, Japan Science and Technology Agency (JST) (T.N.).

Acknowledgements. This project was initiated by the discussions with T.N. and Prof. Dennis Bray in University of Cambridge, and D. Bray advised on the project.

References

1. Corning WC, Dyal JA, Willows AO. 1973 *Invertebrate learning: I. Protozoans through annelids*. New York, NY: Plenum Press.
2. Eisenstein EM. 1975 *Aneural organisms in neurobiology*. New York, NY: Springer.
3. Ball P. 2008 Cellular memory hints at the origins of intelligence. *Nature* **451**, 385. (doi:10.1038/451385a)

4. Bray D. 2009 *Wetware: a computer in every living cell*. London, UK: Yale University Press.
5. Eckert R. 1972 Bioelectric control of ciliary activity. *Science* **176**, 473–481. (doi:10.1126/science.176.4034.473)
6. Naitoh Y. 1974 Bioelectric basis of behavior in protozoa. *Am. Zool.* **14**, 883–893. (doi:10.1093/icb/14.3.883)
7. Naitoh Y, Sugino K. 1984 Ciliary movement and its control in *Paramecium*. *J. Protozool*. **31**, 31–40. (doi:10.1111/j.1550-7408.1984.tb04285.x)
8. Jennings HS. 1906 *Behavior of the lower organisms*. New York, NY: Columbia University Press.
9. Smith S. 1908 The limits of educability in *Paramœcium*. *J. Comp. Neurol. Psychol*. **18**, 499–510. (doi:10.1002/cne.920180506)
10. Day LM, Bentley M. 1911 A note on learning in *paramecium*. *J. Animal Behavior* **1**, 67–73. (doi:10.1037/h0071290)
11. French JW. 1940 Trial and error learning in *paramecium*. *J. Exp. Psychol*. **26**, 609–613. (doi:10.1037/h0059015)
12. Hanzel TE, Rucker WB. 1972 Trial and error learning in *Paramecium*: a replication. *Behav. Biol*. **7**, 873–880. (doi:10.1016/S0091-6773(72)80180-9)
13. Hinkle DJ, Wood DC. 1994 Is tube-escape learning by protozoa associative learning? *Behav. Neurosci*. **108**, 94–99. (doi:10.1037/0735-7044.108.1.94)
14. Kunita I, Kuroda S, Ohki K, Nakagaki T. 2014 Attempts to retreat from a dead-ended long capillary by backward swimming in *Paramecium*. *Front. Microbiol.* **5**, 270. (doi:10.3389/fmicb.2014.00270)
15. Saigusa T, Tero A, Nakagaki T, Kuramoto Y. 2008 Amoebae anticipate periodic events. *Phys. Rev. Lett*. **100**, 018101. (doi:10.1103/PhysRevLett.100.018101)
16. Nakagaki T, Yamada H, Toth A. 2000 Maze-solving by an amoeba. *Nature* **407**, 470. (doi:10.1038/35035159)
17. Bramstedt F. 1935 Dressurversuche mit *Paramecium caudatum* und *Stylonchia mytilus*. *Z. Vergl. Physiol*. **22**, 490–516.
18. Grabowski U. 1939 Experimentelle Untersuchungen ueber das angebliche Lernvermoegen von *Paramecium*. *Z. Tierphyschol.* **2**, 265–282. (doi:10.1007/BF00572723)
19. Levandowsky M, Hutner SH (eds). 1979 *Biochemistry and physiology of protozoa*, 2nd edn, vol. 1. New York, NY: Academic Press Inc.
20. Machemer H, Ogura A. 1979 Ionic conductances of membranes in ciliated and deciliated *Paramecium*. *J. Physiol*. **296**, 49–60. (doi:10.1113/jphysiol.1979.sp012990)
21. Machemer H. 1989 Cellular behaviour modulated by ions: electrophysiological implications. *J. Protozool*. **36**, 463–487. (doi:10.1111/j.1550-7408.1989.tb01082.x)
22. Tominaga T, Naitoh Y. 1994 Comparison between thermoreceptor and mechanoreceptor currents in *Paramecium caudatum*. *J. Exp. Biol*. **189**, 117–131.
23. Dunlap K. 1977 Localization of calcium channels in *Paramecium caudatum*. *J. Physiol.* **271**, 119–133. (doi:10.1113/jphysiol.1977.sp011993)
24. Nakaoka Y, Tokui H, Gion Y, Inoue S, Oosawa F. 1982 Behavioral adaptation of *Paramecium caudatum* to environmental temperature: the effect of cell density. *Proc. Jpn Acad. B* **58**, 213–217. (doi:10.2183/pjab.58.213)
25. Oosawa F. 1975 Effect of field fluctuation on a macromolecular system. *J. Theor. Biol*. **52**, 175–186. (doi:10.1016/0022-5193(75)90049-1)
26. Majima T. 1970 Membrane potential fluctuation in *paramecium*. *Biophys. Chem*. **11**, 101–108. (doi:10.1016/0301-4622(80)85012-5)
27. Oosawa F. 2001 Spontaneous signal generation in living cells. *Bull. Math. Biol*. **63**, 643–654. (doi:10.1006/bulm.2001.0236)
28. Oosawa F. 2007 The spontaneous activity of living cells. *Biosystems* **88**. 191–201. (doi:10.1016/j.biosystems.2006.05.006)
29. Hennessey TM, Kung C. 1985 Slow inactivation of the calcium current of *Paramecium* is dependent on voltage and not internal calcium. *J. Physiol*. **365**, 165–179. (doi:10.1113/jphysiol.1985.sp015765)
30. Nam SW *et al.* 2009 N-Methyl-d-Aspartate receptor-mediated chemotaxis and Ca^{2+} singnaling in *Tetrahymena pyriformis*. *Protist* **160**, 331–342. (doi:10.1016/j.protis.2008.10.005)
31. Ramoino P, Candiani S, Pittaluga AM, Usai C, Gallus L, Ferrando S, Milanese M, Faimali M, Bonanno G. 2014 Pharmacological characterization of NMDA-like receptors in the single-celled organism *Paramecium primaurelia*. *J. Exp. Biol*. **217**, 463–471. (doi:10.1242/jeb.093914)
32. Keener J, Sneyd J. 1998 *Mathematical physiology*, pp. 136–142. New York, NY: Springer.